



**HAL**  
open science

## Small, medium and large shock waves for non-equilibrium radiation hydrodynamics

Corrado Mascia

► **To cite this version:**

Corrado Mascia. Small, medium and large shock waves for non-equilibrium radiation hydrodynamics. Physica D: Nonlinear Phenomena, 2013, 245, pp.46-56. hal-00669787

**HAL Id: hal-00669787**

**<https://hal.science/hal-00669787>**

Submitted on 13 Feb 2012

**HAL** is a multi-disciplinary open access archive for the deposit and dissemination of scientific research documents, whether they are published or not. The documents may come from teaching and research institutions in France or abroad, or from public or private research centers.

L'archive ouverte pluridisciplinaire **HAL**, est destinée au dépôt et à la diffusion de documents scientifiques de niveau recherche, publiés ou non, émanant des établissements d'enseignement et de recherche français ou étrangers, des laboratoires publics ou privés.

# Small, medium and large shock waves for non-equilibrium radiation hydrodynamics

February 13, 2012

Corrado MASCIA<sup>1</sup>

**Abstract.** We examine the existence of shock profiles for a hyperbolic-elliptic system arising in radiation hydrodynamics. The algebraic-differential system for the wave profile is reduced to a standard two-dimensional form that is analyzed in details showing the existence of heteroclinic connection between the two singular points of the system for any distance between the corresponding asymptotic states of the original model. Depending on the location of these asymptotic states, the profile can be either continuous or possesses at most one point of discontinuity. Moreover, a sharp threshold relative to presence of an internal absolute maximum in the temperature profile –also called Zel’dovich spike– is rigorously derived.

**Keywords.** Shock profiles; Radiating gases; Hyperbolic-elliptic systems.

**2010 AMS subject classifications.** 76L05 (35L67, 35M30, 35Q31)

## 1. INTRODUCTION

Fluid dynamics equations support a class of special and significant solutions known as shock waves. These describe physical phenomena consisting in an abrupt transition from one state to another, that, in the simplest setting, are described by a single jump connecting two different states and propagating, in first approximation, with constant speed. In formulas, these corresponds to special solutions of the system under consideration having the form

$$w(x, t) = W(x - ct) \quad W(\pm\infty) = W_{\pm},$$

where  $w$  denotes the state variable,  $W$  the shock profile,  $c$  the velocity and  $W_{\pm}$  the asymptotic states. The difference  $[W] := W_+ - W_-$  and its length are generally used to distinguish between small,  $|W_+ - W_-| \rightarrow 0$ , and large shocks,  $|W_+ - W_-| \rightarrow \infty$ .

In the relevant case of the Euler equations for gasdynamics in one space dimension, obtained considering the conservation of mass, momentum and energy and neglecting higher order effect as viscosity, capillarity, and thermal conductivity, traveling wave solutions propagate with a velocity dictated by the Rankine–Hugoniot condition. Moreover, they have piecewise constant profiles with a single jump point, where physical entropy increases along the discontinuity. The persistence of the presence of waves when considering also higher order effects has been considered by several authors and in different context. Among others, let us quote the classical reference [4] where the existence of shock layers for a model taking into account both viscosity and heat conductivity.

---

<sup>1</sup>Dipartimento di Matematica “G. Castelnuovo”, Sapienza – Università di Roma, P.le Aldo Moro, 2 - 00185 Roma (ITALY), [mascia@mat.uniroma1.it](mailto:mascia@mat.uniroma1.it) AND Istituto per le Applicazioni del Calcolo, Consiglio Nazionale delle Ricerche (associated in the framework of the program “Intracellular Signalling”)

The present article fits into the strand of radiation hydrodynamics (see [13, 16]). Specifically, we consider the classic Euler equations coupled with an elliptic equation for an additional variable describing the intensity of radiation; precisely, we deal with the hyperbolic-elliptic system

$$(1) \quad \begin{cases} \partial_t \rho + \partial_x(\rho u) = 0, \\ \partial_t(\rho u) + \partial_x(\rho u^2 + p) = 0, \\ \partial_t(\rho E) + \partial_x(\rho E u + p u - \sigma_s^{-1} \partial_x n) = 0, \\ \partial_x^2 n = \tau^2(n - g(\theta)) \end{cases}$$

where the variables  $\rho, u, p, E$  and  $\theta$  represent density, velocity, pressure, specific total energy and temperature of the fluid under consideration. The additional variable  $n$  describes the specific intensity of radiation and the coupling is governed by the constants  $\tau, \sigma_s$  and by the function  $g = g(\theta)$ .

The model (1) derives from a hyperbolic–kinetic system where the radiation is described by an additional variable for the photons density satisfying a transport equation with interaction kernel given by the Stefan–Boltzmann law. System (1) is obtained in the non-relativistic limit (speed of light tending to  $+\infty$ ) and the variable  $n$  is an average of the photon density. The elliptic equation for the variable  $n$  emerges from the assumption that the variable  $n$  is linked with the temperature by the integral relation

$$n(x, t) = \int_{\mathbb{R}} g(\theta(y, t)) K(|x - y|) dy$$

with an exponential kernel  $K(s) = \frac{1}{2} \tau e^{-\tau s}$ . Details on the derivation of asymptotic regimes as the one described by (1) can be found in [1, 5, 12].

As usual, the pressure is considered a function of density and temperature,  $p = p(\rho, \theta)$  and the specific total energy  $E$  is given by

$$E = \frac{1}{2} u^2 + e$$

where the internal energy  $e$ , in general, may depend on  $\rho$  and  $\theta$ ,  $e = e(\rho, \theta)$ . Precisely, we concentrate on the case of polytropic perfect gases; this amounts in considering the functions  $p, e, g$  given by the formulas

$$(2) \quad p = R \rho \theta, \quad e = \frac{R}{\gamma - 1} \theta, \quad g(\theta) = \sigma \theta^\alpha$$

where  $\gamma > 1$  is the adiabatic constant ( $\gamma = 5/3$  for monoatomic gases, and  $\gamma = 7/5$  for diatomic gases),  $R > 0$  the perfect gas constant,  $\sigma$  the Stefan–Boltzmann constant and  $\alpha = 4$ .

Existence of shock profiles in the context of radiation hydrodynamics have been considered for many years. In [7, 16, 13], a formal analysis is performed concentrating on specific ranges for the asymptotic states relative to the size of the shock and the strength of the radiation effect. More recently, rigorous proof has been presented:

– for a simplified model, known as the Hamer model, consisting of a single scalar conservation law coupled with an elliptic equation, mimicking the form of the system (1) (small and smooth shocks [15], general and possibly discontinuous shocks [8, 9, 10]);

– for systems, both for the special form (1) (small and smooth shocks [11], large and discontinuous shocks [2]) and for general hyperbolic–elliptic systems (small shocks and linear coupling [9], small shocks and nonlinear coupling [10]).

Here, we contribute to the exploration of system (1) showing existence of shock profiles for all of the possible regimes: small, medium and large size. Apart for the requests on the form of constitutive functions  $p$ ,  $e$  and  $g$ , the unique assumption is that the asymptotic states connected by the shock profile determine an admissible shock wave for the corresponding reduced hyperbolic system.

**Theorem 1.1.** *Assume (2) with  $R > 0, \gamma > 1, \alpha > 0$ . Let the triples  $(\rho_{\pm}, u_{\pm}, \theta_{\pm})$  and the constant  $c \in \mathbb{R}$  be such that the Rankine–Hugoniot conditions*

$$c[\rho] = [\rho u], \quad c[\rho u] = [\rho U^2 + p], \quad c[\rho E] = [\rho E U + p U]$$

*are satisfied, together with the entropy condition for 1-shocks*

$$c + \sqrt{\gamma \theta_-} < u_-, \quad c < u_+ < c + \sqrt{\gamma \theta_+}$$

*Then system (1) supports a shock wave, that is solution of the form*

$$(\rho, u, \theta, n) = (\rho_{\pm}, u_{\pm}, \theta_{\pm}, n_{\pm})(x - ct)$$

*such that  $(\rho, u, \theta, n, \partial_x n)(\pm\infty) = (\rho_{\pm}, u_{\pm}, \theta_{\pm}, g(\theta_{\pm}), 0)$ .*

*The profile is unique up to translations and possesses at most one discontinuity point; if this is the case, all of the variables  $\rho, u$  and  $\theta$  have a jump at such point.*

Once the existence of the shock waves is established, it is meaningful to determine qualitative properties of the profile and, precisely, its smoothness and its monotonicity. To this aim, we introduce the velocities  $U_{\pm} := u_{\pm} - c$ , giving the speed of propagation of the asymptotic states relatively to a reference frame joint with the shock. The following statement concerns with the regularity of the profile, giving sufficient conditions for the presence of a jump point, and with the monotonicity of the component of the profile. Both they are stated in term of the key parameter given by the ratio between the velocity jump of the shock, i.e.  $|u_+ - u_-| = |U_+ - U_-|$ , and the average velocity given by the arithmetic mean  $(U_+ + U_-)/2$ . Precisely, we consider the parameter

$$\delta := \frac{|U_+ - U_-|}{U_c} \quad \text{where} \quad U_c := \frac{U_+ + U_-}{2},$$

so that the measure of the shock size is always normalized with respect to the average speed of propagation of the asymptotic states relatively to the shock velocity.

**Theorem 1.2.** *Assume (2) with  $R > 0, \gamma > 1, \alpha > 0$ .*

**i.** *If  $\gamma < 2$ , the profile of the shock wave determined in Theorem 1.1 is discontinuous in the components  $\rho, u$  and  $\theta$  if*

$$\delta \geq \delta_{jump} := \frac{2(\gamma - 1)}{\gamma}.$$

ii. The component  $\rho$  and  $u$  of the profile of the shock determined in Theorem 1.1 are always monotone, while the temperature profile is monotone if and only if  $\gamma < 3$  and

$$\delta \leq \delta_{spike} := \frac{\gamma - 1}{\gamma}.$$

If this condition is not satisfied, the temperature profile has a single internal absolute maximum point that can be either attained at the jump point or at some point of regularity.

As a consequence of the entropy conditions, the value of  $\delta$  belong always to the interval  $(0, 2/\gamma)$ . For  $\gamma \in (1, 3)$ , there holds  $0 < \delta_{spike} < \delta_{jump} < 2/\gamma$ , hence, depending on the range of values of the parameter  $\delta$ , we can distinguish three different type of temperature profiles: monotone and continuous, non-monotone and continuous, non-monotone and discontinuous.

The smallness of the parameter  $\delta$  is not equivalent to the one of the shock strength  $|(\rho_+, U_+, \theta_+) - (\rho_-, U_-, \theta_-)|$ . Indeed, from the Rankine–Hugoniot relations, we infer

$$[\rho] = \frac{4\rho_{\pm}U_{\pm}}{4 - \delta^2} \frac{\delta^2}{[u]}, \quad [\theta] = \frac{\gamma - 1}{\gamma R} \frac{[u]^2}{\delta}$$

and thus the small shock assumption corresponds to the requests

$$[u]^2 \ll \delta \ll |[u]|^{1/2} \ll 1.$$

As showed in [11, 10], in this limiting regime, the profile is smooth. Theorem 1.2 gives the necessary condition  $\delta < \delta_{jump}$  for such regularity. An additional condition is also obtained during the proof, see (26), and not reported here because of its scarce readability.

With respect to previous rigorous results on radiative shocks Theorems 1.1 and 1.2 can be considered as conspicuous improvements. By restricting the attention to a specific system, we can implement a strategy closely resembling the one considered in [9, 10] passing from a local study for small shocks to a global analysis for any possible shock size. With respect to [2], where the case of large shocks is considered, in addition to the removal of the size assumption, we reduce drastically the assumption on the data of the problem.

As usual, the proof is based on the analysis of the system of ordinary differential equations obtained by looking for traveling wave solutions to (1). Taking advantage of the conserved quantity, such fifth-order system can be reduced to a second-order one. The main original ingredient in the proof resides in the choice of the variable selected for the reduction. The analysis in [2, 7, 8, 11] is based on the study of the second-order differential equation solved by the velocity variable  $u$ ; differently, in [9, 10], it is preferred to consider the second-order equation for the radiation variable  $n$ . Here, we decide for the somewhat intermediate approach given by considering the first-order system for velocity  $u$  and radiation  $n$ . Such system is transformed in the standard form, that is common to the one valid for the Hamer model, and the subsequent analysis consists in a detailed study of such a prototypical system, for which the existence of a heteroclinic orbit, possibly discontinuous is proved (see Proposition 3.4). Theorems 1.1 and 1.2 descend from Proposition 3.4 and the construction of the heteroclinic orbit for the reduced system.

The paper is organized as follows. In Section 2, we show how to reduce the original problem for the radiation hydrodynamics model (1) to a standard form. For completeness, we also present how the same strategy operates in the case of the Hamer model. Section 3 is devoted to the analysis of the system in standard form and to the construction of heteroclinic orbits connecting the two singular points. In Section 4, we resume to the original model, interpreting the construction of the previous Section in term of the hydrodynamics variables. Finally, we draw conclusions in Section 5, pointing at some possible appealing directions for future research in the subject.

## 2. SCALING DOWN TO THE REDUCED SYSTEM

Due to the conservation structure, the system of ordinary differential equations for the profile of the radiative shock under investigation can be reduced to a first order system for a two-dimensional variable. The aim of this Section is to show that such a reduced system has the form

$$(3) \quad \frac{dx}{d\xi} = \frac{1}{\nu} \frac{G(x) - y}{x}, \quad \frac{dy}{d\xi} = \frac{1}{2} \nu (1 - x^2).$$

for an appropriate function  $G$  and positive parameter  $\nu$ . The same procedure can be applied to a simpler system given by the coupling of a scalar conservation law with an elliptic equation. For pedagogical reasons, we first present this simpler situation and postpone the discussion of the Euler system with radiation (1). Since the two derivations of (3) are independent, the reader may skip the first part and move directly to the case of radiation hydrodynamics.

**Hamer model.** Given smooth functions  $f$  and  $g$ , let us consider the hyperbolic-elliptic system, known as **Hamer model** (see [6] and descendants)

$$(4) \quad \begin{cases} \partial_t u + \partial_x (f(u) - \partial_x n) = 0, \\ \partial_x^2 n - n + g(u) = 0. \end{cases}$$

For convex fluxes  $f$ , the hyperbolic scalar conservation law obtained by disregarding the coupling term  $\partial_x n$  possesses shock waves connecting states  $u_{\pm}$  if and only if  $u_+ < u_-$ . Such waves have a piecewise constant profile with a single jump point and propagates with a speed  $c$  that is given by the Rankine–Hugoniot condition, *viz.*

$$(5) \quad c = \frac{[f(u)]}{[u]} = \frac{f(u_+) - f(u_-)}{u_+ - u_-}$$

In analogy, we look for traveling fronts  $(u, n) = (u, n)(x - ct)$  that solves (4) and satisfy the asymptotic conditions

$$u(\pm\infty) = u_{\pm} \quad n(\pm\infty) = g(u_{\pm}), \quad \partial_x n(\pm\infty) = 0.$$

Apart for the requests  $u_+ < u_-$  and  $c$  given by (5), we also assume

$$(6) \quad [g] := g(u_+) - g(u_-) < 0.$$

Setting  $\xi = x - ct$ , the couple  $(u, n)$  satisfies an algebraic-differential system

$$(7) \quad m = f(u) - f(u_{\pm}) - c(u - u_{\pm}), \quad \frac{dn}{d\xi} = m, \quad \frac{dm}{d\xi} = n - g(u),$$

to be interpreted as a two-dimensional dynamical system along a surface in the three-dimensional space  $(u, n, m)$ .

There are different possible ways to deal with (7), corresponding to different choices of unknown. The approach in [15, 8] consists essentially in deriving a second order differential equation for the variable  $u$ , while the strategy used in [9, 10], dictated by the better regularity properties of the variable  $n$ , corresponds to consider the couple  $(n, m)$ . Differently, we deal with (7) in a way that is somewhat in between the two and we look for a reduced system for the couple  $(u, n)$ . This method avoids the necessity to invert the relation  $m = f(u) - f(u_{\pm}) - c(u - u_{\pm})$ , but it has the drawback of the possible presence of jumps of the trajectory.

Differentiating the first equation, we get

$$\frac{dm}{d\xi} = (f'(u) - c) \frac{du}{d\xi},$$

so that system (7) is completely described by the reduced system

$$\frac{du}{d\xi} = \frac{n - g(u)}{f'(u) - c}, \quad \frac{dn}{d\xi} = f(u) - f(u_{\pm}) - c(u - u_{\pm}).$$

In the case of Burgers equation, i.e.  $f(u) = \frac{1}{2}u^2$ ,  $c = (u_+ + u_-)/2$ ,

$$(8) \quad \frac{du}{d\xi} = \frac{n - g(u)}{u - c}, \quad \frac{dn}{d\xi} = \frac{1}{2}(u - u_-)(u - u_+).$$

Introducing the variable  $(x, y)$  related with  $(u, n)$  by

$$u = \frac{1}{2} \left\{ [u]x + u_- + u_+ \right\} \quad \text{and} \quad n = \frac{1}{2} \left\{ [g]y + g(u_-) + g(u_+) \right\},$$

where  $[u] = u_+ - u_- < 0$ , system (8) takes the form (3) where

$$\nu := -\frac{1}{2} \frac{[u]^2}{[g]} \quad \text{and} \quad G(x) := \frac{2(g \circ u)(x) - g(u_-) - g(u_+)}{[g]}.$$

The function  $G$  and the parameter  $\nu$  have to be regarded as functions of the asymptotic states  $u_{\pm}$  or, equivalently, of the values  $[u]$  and  $c$ . By definition, for any choice of  $u_{\pm}$  there hold  $G(\pm 1) = \pm 1$ .

**Example 2.1.** For a linear term  $g$ , viz.  $g(u) = \sigma u$  for some  $\sigma > 0$ , the expressions for  $\nu$  and  $G$  are

$$\nu = -\frac{1}{2\sigma} [u] \quad \text{and} \quad G(x) = x.$$

In the quadratic case,  $g(u) = \sigma u^2$ ,  $\sigma > 0$ , we obtain

$$\nu = -\frac{1}{4\sigma} \frac{[u]}{c} \quad \text{and} \quad G(x) = x - \frac{1}{4} \frac{[u]}{c} (1 - x^2).$$

where  $c = \frac{1}{2}(u_+ + u_-)$ . In this case, both  $\nu$  and  $G$  are homogeneous with respect to the couple  $([u], c)$  and thus system (3) does not vary if the ratio  $[u]/c$  is kept fixed.

In general, for  $g(u) = \sigma u^{\alpha}$  for some exponent  $\alpha > 0$ , the value  $[g]$  is homogeneous of degree  $\alpha$  with respect to  $[u]$  and  $c$ , and, as a consequence, the parameter  $\nu$  is a homogeneous function of degree  $2 - \alpha$  with respect to the couple  $([u], c)$  and  $G$  is homogeneous of degree 0. Explicit expressions for the corresponding  $\nu$  and  $G$  does not seem particularly significant.

Solutions to system (3) may possess eventual discontinuity. At such point,  $y$  is continuous (as a consequence of the continuity of  $n$ ) and, denoting by  $x_\ell$  and  $x_r$  the values of  $x$  at the left and at the right of the jump point, respectively, there hold

$$x_\ell < x_r \quad \text{and} \quad x_\ell + x_r = 0.$$

Solutions to (3) with the above jump conditions will be analyzed in the Section 3.

In the remaining part of the present Section, we show how system (3) emerges also when looking for traveling wave solutions for the radiating Euler system (1).

**Radiation hydrodynamics.** Next, we consider the hyperbolic-elliptic system (1) describing the evolution of a compressible fluid under the effect of radiation. Setting  $\sigma_s^{-1} = 0$ , the first three equations in system (1) reduce to a standard hyperbolic model for compressible fluids. Such system possesses shock solutions, i.e. traveling wave solutions  $W = W(x - ct)$  with piecewise constant profile  $W$  of the form

$$W(\xi) = W_- \chi_{(-\infty, 0)}(\xi) + W_+ \chi_{(0, +\infty)}(\xi).$$

for appropriate states  $W_\pm$  and parameter  $c$ . The shock speed  $c$  is related with the states  $W_\pm$  by means of the Rankine–Hugoniot condition. Precisely, setting  $U = u - c$ , there hold

$$\begin{cases} \rho_- U_- = \rho_+ U_+, \\ \rho_- U_-^2 + p_- = \rho_+ U_+^2 + p_+, \\ \rho_- U_- \left( \frac{1}{2} U_-^2 + e_- \right) + p_- U_- = \rho_+ U_+ \left( \frac{1}{2} U_+^2 + e_+ \right) + p_+ U_+ \end{cases}$$

In the case (2), if  $\rho_\pm U_\pm \neq 0$ , the values  $\theta_\pm$  satisfy the linear system

$$U_+ \theta_- - U_- \theta_+ = \frac{1}{R} U_- U_+ [u], \quad \theta_- - \theta_+ = \frac{\gamma - 1}{2\gamma R} (U_+ + U_-) [u],$$

hence, they can be written as explicit functions of  $U_\pm$

$$\theta_- = \frac{1}{\gamma R} \left( U_c - \frac{1}{2} [u] \right) \left( U_c + \frac{\gamma}{2} [u] \right), \quad \theta_+ = \frac{1}{\gamma R} \left( U_c + \frac{1}{2} [u] \right) \left( U_c - \frac{\gamma}{2} [u] \right)$$

where  $U_c := \frac{1}{2}(U_- + U_+)$ . Note also that, if the jump  $[u]$  is strictly negative, then the jumps  $[\rho]$  and  $[\theta]$  are both strictly positive.

Still taking advantage of (2), entropy conditions in the case of 1-shocks require  $U_\pm, \theta_\pm$  to be such that

$$(9) \quad \sqrt{\gamma \theta_-} < U_-, \quad 0 < U_+ < \sqrt{\gamma \theta_+},$$

which implies  $U_+ < U_-$ , since  $[\theta]$  and  $[u]$  have opposite sign.

For later use, let us set

$$(10) \quad A := \rho_\pm U_\pm, \quad B := \rho_\pm U_\pm^2 + p_\pm \quad C := \rho_\pm U_\pm \left( \frac{1}{2} U_\pm^2 + e_\pm \right) + p_\pm U_\pm.$$

or, equivalently,

$$A := \rho_\pm U_\pm, \quad B := \frac{\gamma + 1}{2\gamma} A (U_- + U_+) \quad C := \frac{\gamma + 1}{2(\gamma - 1)} A U_- U_+.$$

having used (2).

We are interested in determining the existence and the internal structure of traveling wave solutions

$$(\rho, u, \theta, n) = (\rho, u, \theta, n)(x - ct)$$

solutions to (1) such that  $(\rho, u, \theta, n, \partial_x n)(\pm\infty) = (\rho_{\pm}, u_{\pm}, \theta_{\pm}, g(\theta_{\pm}), 0)$ . Plugging the traveling wave ansatz into the system, we get the system of differential equation

$$(11) \quad \begin{aligned} \frac{d}{d\xi}(\rho U) &= 0, & \frac{d}{d\xi}(\rho U^2 + p) &= 0, \\ \frac{d}{d\xi} \left( \rho U \left( \frac{1}{2} U^2 + e \right) + p U - \frac{1}{\sigma_s} \frac{dn}{d\xi} \right) &= 0, & \frac{d^2 n}{d\xi^2} &= \tau^2 (n - g(\theta)) \end{aligned}$$

to be satisfied in the regions where the wave profile is smooth.

The conservative form of the first two equations implies that

$$\rho U = A \quad \text{and} \quad \rho U^2 + p = B$$

all along the trajectory for any weak solution to (11) where  $A$  and  $B$  are given in (10). Thus, there hold

$$(12) \quad \rho = \rho(U) = \frac{A}{U}, \quad p = p(U) = B - AU$$

and system (11) reduces to the algebraic-differential system

$$(13) \quad m = \sigma_s f(U), \quad \frac{dn}{d\xi} = m, \quad \frac{dm}{d\xi} = \tau^2 (n - (g \circ \theta)(U))$$

where, for  $A, B, C$  as in (10),

$$(14) \quad f(U) := -\frac{1}{2} A U^2 + A e(U) + B U - C,$$

and  $e(U) = e(\rho(U), \theta(U))$  with  $\rho(U)$  and  $\theta(U)$  are obtained from (2) and (12). System (13) describes a two-dimensional dynamical system in the three-dimensional space  $(U, n, m)$  along the manifold  $\Sigma$  determined by the algebraic relation  $m = \sigma_s f(U)$ . Using the special form for pressure  $p$  and internal energy  $e$  given in (2), the function  $f$  can be rewritten as

$$(15) \quad f(U) = -\kappa (U - U_+)(U - U_-) \quad \text{where} \quad \kappa := \frac{\gamma + 1}{2(\gamma - 1)} A.$$

If the profile has a jump point at some point, the function  $n$  and its first derivative are forced to be continuous at such point, since the last equation in (13) forces the second derivative of  $n$  to be bounded and measurable. As a consequence, denoting by  $\rho_\ell, U_\ell, \theta_\ell$  and  $\rho_r, U_r, \theta_r$  the values at the left-/right-hand side of the discontinuity, the relation  $f(U_\ell) = f(U_r)$  holds together with the admissibility conditions that read as, in the case of 1-shocks,

$$\sqrt{R\gamma\theta_\ell} < U_\ell, \quad 0 < U_r < \sqrt{R\gamma\theta_r}$$

Because of (15), jumps are admissible if and only if

$$(16) \quad U_c < U_\ell < 2U_c \quad \text{where} \quad U_c := \frac{U_+ + U_-}{2}$$

the corresponding value  $U_r$  being given by  $2U_c - U_\ell$ .

There are different possible ways to deal with (13), corresponding to different choices of unknown. As for the Hamer model, two main approaches have been used: in [7, 11, 2] a second order differential equation for the variable  $U$  is derived, in [9, 10] it has been considered the dynamics for the couple  $(n, m)$ , because of the greater regularity of the variable  $n$ . Here, we proceed by deriving a system for the couple  $(U, n)$ , hence, with the possibility of trajectories that are discontinuous at some point in the first component of the unknowns.

Differentiating with respect to  $\xi$  the equation defining the surface  $\Sigma$  and eliminating the variable  $m$ , we get the reduced two-dimensional system

$$(17) \quad \frac{dU}{d\xi} = \frac{\tau^2}{\sigma_s} \frac{n - (g \circ \theta)(U)}{f'(U)}, \quad \frac{dn}{d\xi} = \sigma_s f(U).$$

Thanks to (2), function  $f$  is the second-order polynomial given in (15) and  $f'(U) = -2\kappa(U - U_c)$ . The final step consists in introducing new coordinates to transform the system in the standard form (3).

Introducing the variable  $(x, y)$  related with  $(U, n)$  by

$$U = U(x) := \frac{1}{2} \{ [u]x + U_- + U_+ \} \quad \text{and} \quad n = n(y) := \frac{1}{2} \{ [g]y + g(\theta_-) + g(\theta_+) \},$$

system (17) becomes

$$\frac{dx}{d\xi} = \frac{\tau^2 [g]}{\sigma_s \kappa [u]^2} \frac{G(x) - y}{x}, \quad \frac{dy}{d\xi} = \frac{\sigma_s \kappa [u]^2}{2[g]} \nu(1 - x^2)$$

where

$$(18) \quad G(x) := \frac{1}{[g]} (2(g \circ \theta \circ U)(x) - g(\theta_-) - g(\theta_+))$$

By rescaling the variable  $\xi$  by setting  $\xi = \tau \zeta$ , we end up with the system (3) where

$$(19) \quad \nu := \frac{\kappa \sigma_s [u]^2}{\tau [g]}.$$

Both function  $G$  and parameter  $\nu$  depends on the values of the asymptotic states of the profile and thus can be regarded as functions of the parameters  $[u]$  and  $U_c$ .

Let us also observe that the function  $\theta \circ U = (\theta \circ U)(x)$  is given by

$$(\theta \circ U)(x) = \frac{1}{R} \left( \frac{\gamma + 1}{\gamma} U_c - U \right) U = \frac{1}{\gamma R} \left( U_c + \frac{1}{2}[u]x \right) \left( U_c - \frac{1}{2}\gamma [u]x \right);$$

thus, there holds

$$\frac{d}{dx}(\theta \circ U)(x) = -\frac{[u]^2}{2R} (x - x_c) \quad \text{where } x_c := -\frac{\gamma - 1}{\gamma} \frac{U_c}{[u]} > 0.$$

As a consequence, if  $g$  is strictly increasing, the function  $G$  has the same monotonicity of  $\theta \circ U$  and it is strictly increasing in  $[-1, 1]$  if and only if  $x > 1$ , that is if and only if

$$|u_+ - u_-| \leq \frac{\gamma - 1}{\gamma} U_c.$$

Otherwise,  $G$  is strictly increasing in  $[-1, x_c]$  and strictly decreasing in  $[x_c, 1]$ .

**Example 2.2.** In the case  $g(\theta) = \sigma \theta$  with  $\sigma > 0$ , the parameter  $\nu$  and the function  $G$  can be computed explicitly

$$\nu = \frac{\kappa \sigma_s [u]^2}{\tau \sigma [\theta]} = \frac{\gamma(\gamma+1) R \sigma_s A}{2(\gamma-1)^2 \tau \sigma} \delta,$$

$$G(x) = \frac{2(\theta \circ U)(x) - \theta_+ - \theta_-}{\theta_+ - \theta_-} = x + \frac{\gamma}{2(\gamma-1)} \delta(1-x^2)$$

Thus, the structure is essentially the same of the Hamer model (4) with a quadratic function  $g$  (see Example 2.1).

Higher powers in the temperature dependence of function  $g$ , i.e.  $g(\theta) = \sigma \theta^\alpha$  with  $\sigma > 0$  and  $\alpha$  a positive integer, give raise to complicate formulas, whose explicit expression is not particularly significant. It is relevant to observe that, being  $\theta \circ U$  a homogeneous function of degree 2 with respect to  $[u]$  and  $U_c$ , the value  $[g]$  is homogeneous of degree  $2\alpha$  and thus  $\nu$  is homogeneous of degree  $2(1-\alpha)$  and  $G$  is homogeneous of degree 0 with respect to the same variables. In particular, when the ratio

$$\delta := -\frac{[u]}{U_c} = \frac{1}{2} \frac{U_- - U_+}{U_- + U_+}$$

is kept fixed the function  $G$  does not change and the parameter  $\nu$  decreases as  $-[u]$  increases if  $\alpha > 1$ .

An eventual discontinuity in the trajectory keeps  $y$  fixed; moreover, if  $x_\ell$  and  $x_r$  denote the values at the left and at the right of the jump, then  $x_r = -x_\ell$  and condition (16) translates into

$$(20) \quad \frac{U_+ + U_-}{U_+ - U_-} < x_\ell < 0.$$

Note that the value  $(U_+ + U_-)/(U_+ - U_-)$  is always strictly smaller than  $-1$ , so that jumps are always allowed if  $x \in [-1, 0)$ .

**Remark 2.3.** The analysis is based on the choice (2), that plays a key-rôle in determining the specific expression (15) for the function  $f$ . For more general expression of pressure  $p$  and internal energy  $e$ , all of the subsequent analysis can still be performed if the function  $f$ , given by formula (14), is strictly concave.

### 3. ANALYSIS OF THE REDUCED SYSTEM

In this Section, we consider piecewise smooth solutions to the system

$$(21) \quad \frac{dx}{d\zeta} = \frac{1}{\nu} \frac{G(x) - y}{x}, \quad \frac{dy}{d\zeta} = \frac{1}{2} \nu (1 - x^2).$$

with  $\nu > 0$  and  $G$  smooth and such that  $G(\pm 1) = \pm 1$ . At any eventual jump point  $\xi$ , we assume that the couple  $(x, y)$  possesses left/right limits, denoted by  $(x_\ell, y_\ell)$  and  $(x_r, y_r)$ , and that

$$x_\ell < x_r, \quad x_\ell + x_r = 0, \quad y_\ell - y_r = 0$$

System (21) has two singular points,  $P_- := (-1, -1)$  and  $P_+ := (+1, +1)$ , and we are interested in the existence of a heteroclinic orbit connecting such that  $(x, y)(\pm\infty) =$

$P_{\pm}$ . Since both critical points  $P_{\pm}$  are saddles, such orbit is obtained by matching the unstable one-dimensional manifold of  $P_-$  with the stable one-dimensional manifold of  $P_+$  (see Lemma 3.1).

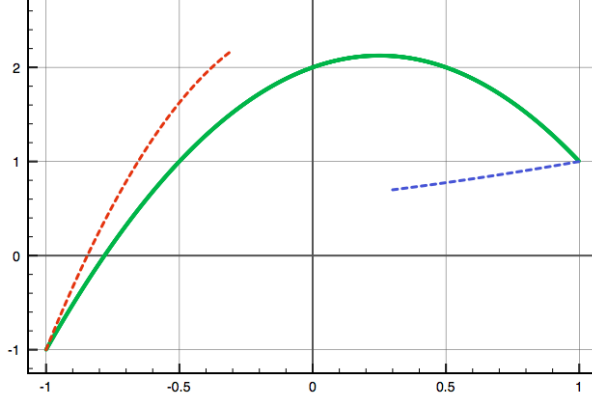


FIGURE 1. The phase plane  $(x, y)$  with the graph of function  $G$  (continuous line) and the unstable/stable manifold of  $P_- = (-1, -1)/P_+ = (1, 1)$  (dashed lines).

The matching may happen either in a continuous or in a discontinuous way, the former case being related with the nature of the system at the singular line  $x = 0$  (see Lemma 3.2).

**Lemma 3.1.** *For any  $\nu > 0$ , the critical points  $P_{\pm}$  are saddles and, denoted by  $\mathcal{U}_-$  the part of unstable manifold of  $P_-$  in  $\{x > -1\}$  and by  $\mathcal{S}_+$  the part of the stable manifold of  $P_+$  in  $\{x < 1\}$ , there exist functions  $\phi_- = \phi_-(x)$  defined in  $[-1, 0]$  and  $\phi_+ = \phi_+(x)$  defined in  $[0, 1]$  both differentiable and strictly monotone increasing, such that*

$$\begin{aligned} \{(x, y) \in \mathcal{U}_- : x \in [-1, 0)\} &= \{(x, y) : x \in [-1, 0), y = \phi_-(x)\} \\ \{(x, y) \in \mathcal{S}_+ : x \in (0, 1]\} &= \{(x, y) : x \in (0, 1], y = \phi_+(x)\} \end{aligned}$$

Moreover,  $\phi_+(x) < G(x)$  for any  $x \in (-1, 0)$  and  $\phi_-(x) > G(x)$  for any  $x \in (0, 1)$ .

*Proof.* The jacobian matrices of (21) at  $P_{\pm}$

$$\frac{1}{\nu} \begin{pmatrix} \pm G'(\pm 1) & \mp 1 \\ \mp \nu^2 & 0 \end{pmatrix},$$

have both determinant equal to  $-1$ ; hence, both points are saddles.

The manifolds  $\mathcal{U}_-$  and  $\mathcal{S}_+$  have tangent directions given by the vectors  $(\mu_-^u, \nu)$  and  $(-\mu_+^s, \nu)$ , respectively, where

$$\mu_-^u := \frac{2\nu}{G'(-1) + \sqrt{G'(-1)^2 + 4\nu^2}}, \quad \mu_+^s := -\frac{2\nu}{G'(1) + \sqrt{G'(1)^2 + 4\nu^2}},$$

Thus, if  $G'(-1) \leq 0$ ,  $\mathcal{U}_-$  lies in the region  $\{(x, y) : y > G(x)\}$  in a neighborhood of  $P_-$ ; similarly, if  $G'(1) \leq 0$ ,  $\mathcal{S}_+$  lies in the region  $\{(x, y) : y < G(x)\}$  in a neighborhood of  $P_+$ .

If  $G'(\pm 1) > 0$ , since  $\mu_-^u < \nu/G'(-1)$  and  $-\mu_+^s < \nu/G'(1)$ , for  $x \in (-1, 1)$ , the manifold  $\mathcal{U}_-$  lies in the region  $\{(x, y) : y > G(x)\}$  and the manifold  $\mathcal{S}_+$  in the region

$\{(x, y) : y < G(x)\}$  in a neighborhood of  $P_-$  and  $P_+$ , respectively. Since  $\Omega_- := \{(x, y) : x \in (-1, 0), y > G(x)\}$  is positively invariant and  $\Omega_+ := \{(x, y) : x \in (0, 1), y < G(x)\}$  is negatively invariant, the  $\mathcal{U}_-$  is described in  $\Omega_-$  by a curve  $y = \phi_-(x)$  and the manifold  $\mathcal{S}_+$  is described in  $\Omega_+$  by a curve  $y = \phi_+(x)$ . Moreover, both functions are monotone increasing with respect to  $x$  since the corresponding derivatives, given by

$$(22) \quad \frac{d}{dx}\phi_{\pm}(x) = \frac{\nu^2 x(1-x^2)}{2(G(\phi) - x)},$$

do not vanish in the interior of  $\Omega_-$  and  $\Omega_+$  respectively. Moreover, because of (22), the functions  $\phi_{\pm}$  cannot have vertical asymptotes in the regions  $(-1, 0)$  and  $(0, 1)$ , respectively; therefore, they are well defined in  $(-1, 0)$  and  $(0, 1)$ , respectively.  $\square$

For a better understanding of the behavior of the curves  $\phi_{\pm}$  at  $x = 0$ , we consider the half plane  $x > 0$  and rescale the independent variable by setting

$$x(\zeta) \frac{d}{d\zeta} = \frac{d}{d\eta}$$

so that (21) takes the form

$$(23) \quad \frac{dx}{d\eta} = \frac{1}{\nu} (G(x) - y), \quad \frac{dy}{d\eta} = \frac{1}{2} \nu x(1-x^2).$$

**Lemma 3.2.** *Assume  $G'(0) \neq 0, 2\nu^2$ . The critical point  $P_0 = (0, G(0))$  of system (23) is an attractive spiral if  $G'(0) < 0$ , a repulsive spiral if  $0 < G'(0) < 2\nu^2$  and a source if  $2\nu^2 < G'(0)$ . In the latter case, there exists  $x_+ \in (0, 1]$  and a monotone increasing function  $\psi_+ = \psi_+(x)$  defined in  $[0, x_+]$  such that the fast unstable trajectory of  $P_0$  in the region  $\Omega_+ = \{x \in (0, 1), y < G(x)\}$  is given by  $(x, \psi_+(x))$ .*

*Proof.* The jacobian matrix at the singular point  $P_0 := (0, G(0))$

$$\frac{1}{\nu} \begin{pmatrix} G'(0) & -1 \\ \nu^2/2 & 0 \end{pmatrix},$$

has real eigenvalues if and only if  $G'(0)^2 - 2\nu^2 > 0$ . In the opposite case, both eigenvalues have real parts of the same sign of  $G'(0)$ . If  $2\nu^2 < G'(0)^2$ , the eigendirections are given by  $(2\mu_0^{\pm}, \nu)$  where

$$\mu_0^{\pm} = \frac{G'(0) \pm \sqrt{G'(0)^2 - 2\nu^2}}{2\nu}$$

Since

$$0 < \frac{\nu}{2\mu_0^+} < \frac{\nu}{2\mu_0^-} < G'(0)$$

the principal directions of the critical point  $(0, G(0))$  both lies into the region  $y < G(x)$  for  $x > 0$ . The fast unstable direction, corresponding to the eigenvalue  $\mu_0^+$ , is uniquely determined and, while lying in  $\Omega_+$ , is the graph of a monotone increasing function  $\psi_+ = \psi_+(x)$ .  $\square$

**Remark 3.3.** If the function  $G$  does not depend on the parameter  $\nu$  the vector field in (23) is a rotated vector field in the sense of Duff [3] in the regions  $\Omega_{\pm}$ , as a consequence of the equality

$$\det \begin{pmatrix} F & G \\ \partial_{\nu} F & \partial_{\nu} G \end{pmatrix} = \frac{1}{\nu} (G(x) - y) x(1 - x^2)$$

(for the analysis of rotated vector field, see also [14]). Thus, the graphs of the function  $\psi_{+}$  rotates anticlockwise as  $\nu$  increase and the map  $\nu \mapsto x_{+}^{\nu}$  is monotone decreasing with respect to  $\nu$ . Moreover, there exists a critical value  $\bar{\nu}_{+}$  such that  $x_{+}^{\nu} = 1$  for  $\nu < \bar{\nu}_{+}$  and  $x_{+}^{\nu} < 1$  for  $\nu > \bar{\nu}_{+}$ .

From Examples 2.1 and 2.2, it is readily seen that the eventuality of a function  $G$  independent on  $\nu$  is rarely verified in concrete cases. Nevertheless, in the case of radiation hydrodynamics, the function  $G$  does not vary if the ratio  $\delta = -[u]/U_c$  is kept fixed. Thus the properties of the rotated vector fields return to be useful in the analysis of variations of the heteroclinic orbit connecting  $P_{-}$  and  $P_{+}$  when varying the asymptotic states  $U_{\pm}$  keeping  $\delta$  fixed.

A result analogous to Lemma 3.2 holds on the side  $x < 0$ , the main difference being related to the fact that the rescaling of the independent variable changes the orientation of the trajectories. In particular, we can state that, for  $2\nu^2 < G'(0)$ , there exists  $x_{-} \in [-1, 0)$  and a monotone increasing function  $\psi_{-} = \psi_{-}(x)$  defined in  $[x_{-}, 0]$  such that the fast stable trajectory of  $P_0$  in the region  $\Omega_{-} = \{x \in (0, 1), y < G(x)\}$  is given by  $(x, \psi_{-}(x))$ .

**Proposition 3.4.** *Let  $\nu > 0$  and  $G \in C^1([-1, 1])$  be such that  $G(\pm 1) = 0$ . Then there exists a heteroclinic orbit connecting  $P_{-}$  with  $P_{+}$ . Such orbit possesses at most a single jump, and such discontinuity is actually present if one of the following conditions is satisfied*

$$(24) \quad G(0) \leq -1, \quad \text{or} \quad 1 \leq G(0), \quad \text{or} \quad G'(0) < 2\nu^2.$$

*Finally, if  $G'(0) > 0$  the trajectory of the heteroclinic orbit is unique.*

*Proof.* 1. The trajectories  $(x, \phi_{\pm}(x))$ , defined in Lemma (3.1), converge to the  $y$ -axis at a finite value of  $\zeta$ . Indeed, there holds

$$\zeta - \zeta_0 = \int_{x(\zeta_0)}^0 \frac{dx}{dx/d\zeta} = \nu \int_{x(\zeta_0)}^0 \frac{x}{G(x) - \phi_{\pm}(x)} dx.$$

The latter integral is finite if  $\phi_{\pm}(0) \neq G(0)$ . If  $\phi_{\pm}(0) = G(0)$ , then  $\phi'_{\pm}(0) \neq G'(0)$  as can be seen from the explicit expression of the principal directions of the singular point  $P_0$  of the rescaled system (23) (see Lemma 3.2). Thus, the function  $x/(G(x) - \phi_{\pm}(x))$  is integrable in small neighborhoods of 0.

2. If  $\phi_{-}(0) = \phi_{+}(0) = G(0)$ , the conjunction of the two orbits  $\phi_{-}$  and  $\phi_{+}$  furnishes the heteroclinic orbit connecting  $P_{-}$  and  $P_{+}$ . In this case, the profile of the corresponding traveling wave is continuous.

3. To complete the proof of the first part of the statement, we assume that either  $\phi_{-}(0) \neq G(0)$  or  $\phi_{+}(0) \neq G(0)$ . Denoted by  $\psi_{\pm}(y)$  the inverse functions of  $\phi_{\pm}$  defined in

$[-1, \phi_-(0)]$  and  $[\phi_+(0), 1]$ , respectively, let us consider the function

$$h(y) := \psi_+(y) + \psi_-(y) \quad y \in [\phi_+(0), \phi_-(0)].$$

Then, by the properties of  $\phi_{\pm}$ , the function  $h$  is strictly increasing and

$$h(\phi_+(0)) := \psi_-(\phi_+(0)) < 0 < \psi_+(\phi_-(0)) = h(\phi_-(0)).$$

Hence, by continuity of  $h$ , there exists a single value  $y_c$  such that  $h(y_c) = 0$ . The connection of the trajectory  $\phi_-$ , truncated at  $x = \psi_-(y_c)$ , and  $\phi_+$ , truncated at  $x = \psi_+(y_c)$  gives the desired heteroclinic orbit.

4. Any of the conditions in (24) implies that one of the trajectories  $\phi_{\pm}$  does not pass through the point  $(0, G(0))$ . Indeed, if  $G(0) \leq -1$ , since the function  $\phi_-$  is monotone increasing, then  $\phi_-(0) > -1 \geq G(0)$ . Similarly, if  $1 \leq G(0)$ , then  $\phi_+(0)$  is strictly greater than  $G(0)$ . Finally, if  $G'(0) < 2\nu^2$ , the point  $P_0$  is a spiral for the rescaled system (23) and no monotone trajectory is allowed to get onto it.

5. To complete the proof, it is sufficient to observe that more can one jump may appear only if there are smooth solutions of (21) passing from the positive side  $\{x > 0\}$  to the negative side  $\{x < 0\}$ . Because of the structure of the vector field defining the system, the corresponding eventual trajectories should pass through the point  $P_0 = (0, G(0))$ , but, in the case  $G'(0) > 0$ , the singular point  $P_0$  is repulsive on  $\{x > 0\}$  and attractive on  $\{x < 0\}$  so that no transition from positive to negative values of  $x$  is possible.  $\square$

**Remark 3.5.** In the case  $G'(0) \leq 0$ , the system (21) possesses trajectories passing through the point  $(0, G(0))$  and going from the region  $x > 0$  to the region  $x < 0$ . Thus, in principle, solutions may have more than a single jump point and we cannot exclude that there exists also other possible orbits with the same asymptotic states. In the concrete case of application of Proposition 3.4 to (4) and (1) the condition  $G'(0) > 0$  is satisfied.

#### 4. BACK TO RADIATION HYDRODYNAMICS

Next, let us analyze the system (21) and the properties of the corresponding heteroclinic orbits in the case of radiation hydrodynamics as derived in Section 2. For the reader convenience, let us recall the formulas

$$G(x) := \frac{1}{[g]} (2(g \circ \theta \circ U)(x) - g(\theta_-) - g(\theta_+)) \quad \text{and} \quad \nu := \frac{\kappa \sigma_s [u]^2}{\tau [g]}.$$

(see formulas (18)–(19)). As stated in the Introduction, we introduce the key-parameter  $\delta := -[u]/U_c$ , so that the expression of the compound function  $(\theta \circ U) = (\theta \circ U)(x)$  becomes

$$(25) \quad (\theta \circ U)(x) = \frac{U_c^2}{\gamma R} \left(1 - \frac{1}{2} \delta x\right) \left(1 + \frac{1}{2} \gamma \delta x\right),$$

that describes the values of temperature as a function of the auxiliary variable  $x$ .

We concentrate on a series of significant issues:

- to determine threshold for the presence/absence of discontinuities;
- to analyze the monotonicity of the temperature profiles;

- to study the regimes  $\delta \rightarrow 0$  and  $\delta \rightarrow 2/\gamma$ ;
- to show a short collection of numerical experiments.

At the end of the Section, for completeness, we also mention how the properties of the reduced system (21) translate in the case of the Hamer model.

**Discontinuous profiles.** As stated in Proposition 3.4, profiles of the traveling waves are discontinuous if condition (24) is satisfied. If  $g$  is monotone increasing and  $[g] > 0$ , there hold  $G(0) \leq -1$  if and only if  $(\theta \circ U)(0) \leq \theta_-$  and  $G(0) \geq 1$  if and only if  $\theta_+ \leq (\theta \circ U)(0)$ . Taking advantage of the expression (25), the previous relations can be rewritten as

$$\begin{aligned} G(0) \leq -1 &\iff 1 \leq \left(1 + \frac{1}{2}\delta\right) \left(1 - \frac{1}{2}\gamma\delta\right) \iff \delta \leq \frac{2(1-\gamma)}{\gamma}, \\ G(0) \geq 1 &\iff \left(1 - \frac{1}{2}\delta\right) \left(1 + \frac{1}{2}\gamma\delta\right) \leq 1 \iff \delta \geq \frac{2(\gamma-1)}{\gamma}. \end{aligned}$$

For  $\gamma > 1$  and  $\delta > 0$ , the first condition is never satisfied.

Additionally, there holds

$$G'(0) = -\frac{\gamma-1}{R\gamma} \frac{[u]}{[g]} U_c \frac{dg}{d\theta} \left( \frac{U_c^2}{\gamma R} \right)$$

so that condition  $G'(0) < 2\nu^2$  is equivalent to

$$(26) \quad \frac{M_0}{A^2} U_c \frac{dg}{d\theta} \left( \frac{U_c^2}{\gamma R} \right) < -\frac{[u]^3}{[g]} \quad \text{where} \quad M_0 := \frac{2(\gamma-1)^3}{R\gamma(\gamma+1)^2} \frac{\tau^2}{\sigma_s^2}$$

For  $g(\theta) = \sigma\theta$ , condition (26) becomes

$$\delta > \frac{m_1}{A} \quad \text{where} \quad m_1 := \frac{\sqrt{2}(\gamma-1)^2}{R\gamma(\gamma+1)} \frac{\sigma\tau}{\sigma_s}$$

For  $g$  as in (2) with  $\alpha$  integer greater than 1, the explicit formulas corresponding to the condition (26) become very intricate and they do not seem to be significant. In any case, let us stress that differently with respect to the condition  $G(0) \geq 1$ , that depends only on the relation between the parameter  $\delta$  and the value of the constant  $\gamma$ , constraint  $G'(0) < 2\nu^2$  depends also on the other characteristic parameters of the system.

Summarizing, we can state that the heteroclinic orbit is discontinuous if

$$(27) \quad \delta \geq \delta_{\text{jump}} := \frac{2(\gamma-1)}{\gamma}$$

Note that, if  $\gamma > 2$ , the region in the plane  $(U_c, |[u]|)$  for which this inequality is satisfied does not intersect the attainable region  $\delta < 2/\gamma$ .

**Temperature spikes.** The temperature profile is given by (25) calculated at  $x = x(\zeta)$ , the first component of the heteroclinic orbit of the reduced system (21). Since  $x = x(\zeta)$  is strictly increasing, the monotonicity of the temperature is controlled by the sign of its first derivative

$$\frac{d}{dx}(\theta \circ U)(x) = -\frac{[u]^2}{2R}(x - x_c) \quad \text{where} \quad x_c := \frac{\gamma-1}{\gamma} \frac{1}{\delta}$$

Hence, the profile has a change in monotonicity if and only if

$$(28) \quad \delta > \delta_{\text{spike}} := \frac{\gamma - 1}{\gamma}$$

Such absolute maximum for the temperature is sometime referred to as the Zel'dovich spike. Note that the condition (28) is optimal and depends only on the value of the constant  $\gamma$  (in particular, it does not depend on the specific form of the function  $g$ !). For  $\gamma > 3$ , the condition (28) is not satisfied if  $\delta < 2/\gamma$ , meaning that for such values of  $\gamma$  the temperature profile is always monotone increasing.

The location of the absolute maximum point for  $\theta$  can be either at the jump point, if present, or in a region of regularity of the profile. In the latter case, the maximum of the temperature is attained at  $x = x_c$  and its value is

$$(29) \quad \theta_{\max} := (\theta \circ U)(x_c) = \frac{(\gamma + 1)^2}{4\gamma^2} \frac{U_c^2}{R}$$

If the point of change of monotonicity coincides with the jump point, the values  $\theta_{\max}$  gives only an estimate from above of the maximum values for the temperature. It is particularly relevant to note that the expression of  $\theta_{\max}$  does depend only on  $\gamma$ ,  $R$  and  $U_c$ .

Estimate (29) can be compared with the corresponding one determined in [13] (formula (104.67), p.573) for  $\gamma < 3$

$$\theta_M := (3 - \gamma) \theta_+.$$

By using the expression for  $\theta_+$  in terms of  $U_c$  and  $[u]$ , we obtain

$$\frac{\theta_{\max}}{\theta_M} = \frac{(\gamma + 1)^2}{4\gamma(3 - \gamma)} \frac{1}{(1 - \delta/2)(1 + \gamma\delta/2)}.$$

Since  $\delta \in (0, 2/\gamma)$ , we infer

$$(30) \quad \frac{1}{3 - \gamma} \leq \frac{\theta_{\max}}{\theta_M} \leq \frac{(\gamma + 1)^2}{8(3 - \gamma)(\gamma - 1)}.$$

In the significant cases  $\gamma = 5/3$  and  $\gamma = 7/5$ , the above estimates becomes

$$\gamma = \frac{5}{3} : \quad \frac{3}{4} \leq \frac{\theta_{\max}}{\theta_M} \leq 1 \quad \gamma = \frac{7}{5} : \quad \frac{5}{8} \leq \frac{\theta_{\max}}{\theta_M} \leq \frac{9}{8}.$$

The expression (30) can be rewritten as

$$1 - \frac{2 - \gamma}{3 - \gamma} \leq \frac{\theta_{\max}}{\theta_M} \leq 1 + \frac{(3\gamma - 5)^2}{8(3 - \gamma)(\gamma - 1)},$$

thus, in the regime  $\gamma < 2$ , the first term in this equality chains is strictly smaller than 1 and the last term, apart for the (physical!) case  $\gamma = 5/3$ , the estimate from above is strictly greater than 1.

**Limiting regimes.** The expression (25) shows that  $\theta \circ U$  has the form  $Cp(x; \gamma, \delta)$  with  $C = U_c^2/\gamma R$  and  $p$  a polynomial of degree 2 in  $x$  with coefficients depending only on  $\delta$  and  $\gamma$ . Therefore, in the case of functions  $g$  with the power-law form described in (2), the function  $G$  in the reduced system (3) does not changes if the parameters  $\gamma$  and  $\delta$  are kept fixed. Here, we want to analyze the behavior of the heteroclinic orbits built in Section 3

for  $\delta$  prescribed in the regimes  $\delta \rightarrow 0$  and  $\delta \rightarrow 2/\gamma$ . To this aim, we need to investigate the function  $G$  for such values of  $\delta$  and analyze the variations for the parameter  $\nu$ .

As  $\delta \rightarrow 0$ , formula (25) can be rewritten as

$$(\theta \circ U)(x) = \frac{U_c^2}{\gamma R} \left( 1 + \frac{1}{2}(\gamma - 1) \delta x \right) + o(\delta).$$

and substituting in the definition of  $G$ , we infer

$$G(x) = x + o(1) \quad \delta \rightarrow 0.$$

Thus, the function  $G$  is strictly increasing and the temperature profile is monotone increasing. As  $\delta \rightarrow 2/\gamma$ , the relation (25) becomes

$$(\theta \circ U)(x) = \frac{U_c^2}{\gamma^2 R} (\gamma - x)(1 + x) + o(\delta - 2/\gamma)$$

Thus, we have

$$G(x) = G_{\gamma,\alpha}(x) + o(\delta - 2/\gamma) \quad \delta \rightarrow \frac{2}{\gamma},$$

where

$$G_{\gamma,\alpha}(x) := -1 + 2 \left( \frac{\gamma - x}{\gamma - 1} \cdot \frac{1 + x}{2} \right)^\alpha$$

In this case, the function  $G$  changes its monotonicity if and only if  $1 < \gamma < 3$  and, if this is the case, has an absolute maximum point at  $(\gamma - 1)/2$ ; moreover,  $G(0) > 1$  if and only if  $\gamma < 2$ . In particular, the temperature profile exhibits the Zel'dovich spike.

Next, we examine the parameter  $\nu$  and its behavior for  $\delta$  fixed and either  $[u] \rightarrow 0$  or  $[u] \rightarrow -\infty$  (equivalently, either  $U_c \rightarrow 0$  or  $U_c \rightarrow +\infty$ ). The assumption  $g(\theta) = \sigma \theta^\alpha$  carries also the identity

$$[g] = \sigma(\theta_+ - \theta_-)(\theta_+^{\alpha-1} + \dots + \theta_-^{\alpha-1}) = -C \sigma [u] U_c^{2\alpha-1}$$

for some positive constant  $C$  only on  $\gamma, \delta, R$  and  $\alpha$ . Inserting in the definition of  $\nu$  given in (19), we end up with

$$\nu = \frac{C \delta}{U_c^{2(\alpha-1)}} = \frac{C \delta^{2\alpha-1}}{[u]^{2(\alpha-1)}}$$

for some positive constant  $C$  dependent only on  $\gamma, A = \rho_\pm U_\pm, \sigma, \sigma_a, \sigma_s$ . Hence, for  $\alpha > 1$ ,  $\nu \rightarrow +\infty$  as  $[u] \rightarrow 0$  (or  $U_c \rightarrow 0$ ) and  $\nu \rightarrow 0$  as  $[u] \rightarrow -\infty$  (or  $U_c \rightarrow +\infty$ ). The case  $\alpha = 1$  is different, since  $\nu$  turns to be constant for  $\delta$  fixed (see Example 2.2). For this reason, we only consider the case  $\alpha > 1$ .

As  $[u] \rightarrow +\infty$ , in an appropriate scale, system (3) formally reduces to

$$\frac{dx}{d\zeta} = \frac{G(x) - y}{x}, \quad \frac{dy}{d\zeta} = 0$$

For  $\delta \rightarrow 0$ , such structure forces the unstable manifold  $\mathcal{U}_-$  of  $P_- = (-1, -1)$  and the stable manifold  $\mathcal{S}_+$  of  $P_- = (+1, +1)$  coincide with the graph of the function  $G(x) = x + o(\delta)$ . The corresponding temperature profile is continuous and strictly monotone increasing.

For  $\delta \rightarrow 2/\gamma$ , and  $\gamma < 2$ , then the unstable manifold  $\mathcal{U}_-$  of  $P_- = (-1, -1)$  coincides with the graph of the function  $G_{\gamma,\alpha}$ ; the stable manifold  $\mathcal{S}_+$  of  $P_- = (+1, +1)$  is given by a horizontal segment at height  $y = 1$ . The heteroclinic orbit is obtained by the connection

of such manifold at the (unique) point where the stable manifold  $\mathcal{U}_-$  is at height 1 (see Figure 2, left). Since  $G_{\gamma,\alpha}$  is symmetric with respect to  $x_c = \frac{1}{2}(\gamma - 1)$ , the value  $x_-$  of the jump is equal to  $2x_c - 1 = -(2 - \gamma)$  and the corresponding value  $x_+$  is  $2 - \gamma$ . The maximum of the temperature profile is attained at the jump point if and only if  $x_+$  is greater than or equal to  $x_c$ , that is if and only if  $\gamma \leq 5/3$ .

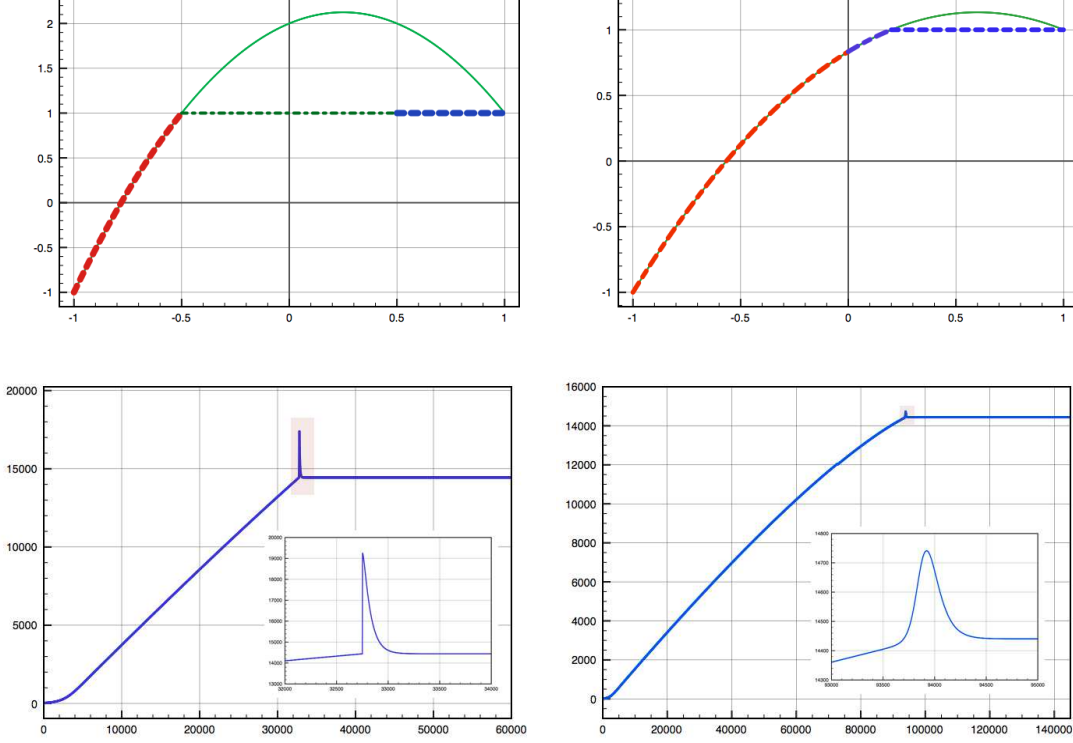


FIGURE 2. Regime  $\delta \rightarrow 2/\gamma$  and  $[u] \rightarrow -\infty$ . Upper line: the phase plane  $(x, y)$  with the graph of the function  $G$  (continuous line) and the heteroclinic orbit connecting the points  $P_- = (-1, -1)$  and  $P_+ = (+1, +1)$  (dashed lines for the continuous part and dashed-dotted line for the jump). Case  $\gamma < 2$  (left) and case  $\gamma > 2$  (right). Lower line: corresponding temperature profiles for the case  $\gamma < 2$  (left) and case  $\gamma > 2$  (right), both with an inside box showing a zoomed version of the spike.

For  $\delta \rightarrow 2/\gamma$ , and  $\gamma \geq 2$ , then the unstable manifold  $\mathcal{U}_-$  of  $P_- = (-1, -1)$  coincides with the graph of the function  $G_{\gamma,\alpha}$  on the interval  $[-1, 0]$ . The stable manifold  $\mathcal{S}_+$  of  $P_+ = (+1, +1)$  is given by the union of the horizontal segment connecting the point  $(\gamma - 2, 1)$  and  $(1, 1)$  and the graph of the function  $G_{\gamma,\alpha}$  for  $x \in [0, \gamma - 2]$  (see Figure 2, right).

For  $[u] \rightarrow 0$ , again in an appropriate scale, system (3) becomes

$$\frac{dx}{d\zeta} = 0, \quad \frac{dy}{d\zeta} = \frac{1}{2}(1 - x^2)$$

In this regime, the limiting dynamics is very simple: the unstable manifold  $\mathcal{U}_-$  of  $P_- = (-1, -1)$  coincides with the vertical half-line  $\{x = -1, y \geq -1\}$  and the stable manifold  $\mathcal{S}_+$  of  $P_+ = (+1, +1)$  with the vertical half-line  $\{x = 1, y \leq 1\}$ . The heteroclinic orbit

is described by a direct jump from  $\mathcal{U}_-$  to  $\mathcal{S}_+$ . The corresponding temperature profile is monotone for  $\delta \rightarrow 0^+$  and non-monotone for  $\delta \rightarrow 2/\gamma$ .

The intermediate cases for  $\nu$  can be deduced qualitatively by noting that, for  $\delta$  fixed and  $\nu$  varying, the system (3) is a rotated vector field, as already observed in Remark 3.3. In particular, as  $\nu$  increases, that is as  $|u_+ - u_-|$  decreases, the trajectory determining the manifolds  $\mathcal{U}_-$  and  $\mathcal{S}_+$  rotate counter clockwise passing from one limiting configuration to the other.

**Numerical experiments.** One of the advantage of the reduced system (3) resides in its simplicity and in the possibility of a numerical approximation of the structure of the radiative profiles by means of a standard solver for ordinary differential equations, complemented with the conditions relative to the eventual jump point. We present here a series of experiments where parameters have been chosen only in part realistic. The value for the adiabatic constant  $\gamma$  is taken equal to  $5/3$  and the constant  $R$  is set equal to 8.31. All of the constants relative to the radiative coupling,  $\sigma, \sigma_s$  and  $\tau$ , are chosen equal to 1. The function  $g$  has the form expressed in (2). As quoted, the realistic exponent  $\alpha$  is 4; nevertheless, for computational advantage, we choose to set  $\alpha = 2$  (the case  $\alpha = 1$  has different behavior in the limiting regimes). Also, to reduce the number of free parameters, we fix  $\rho_-$  at the value 0.1.

Finally, the different cases depend on the choices of the ratio  $\delta$  and values of  $U_c$  (the average of the velocities  $U_{\pm}$  at the left and at the right of the profile). Since  $\gamma = 5/3$ , the thresholds for  $\delta$  are

$$\delta_{\text{spike}} = 0.4 \quad \delta_{\text{jump}} = 0.8 \quad \frac{2}{\gamma} = 1.2$$

Being interested in the behavior for weak/strong radiation and weak/strong shocks we choose  $\delta = 0.6$  (Figure 4, left column) and  $\delta = 1.0$  (Figure 4, right column) and  $U_c$  equal to 10, 50 and 100.

Coherently with the result previously deduced, all of the profiles are non-monotone since both the values of  $\delta$  are taken above the threshold  $\delta_{\text{spike}} = 0.4$ . The choice  $\delta = 1.0$  is also above the threshold  $\delta_{\text{jump}} = 0.8$  and thus the profile are discontinuous. For all of them, the spike coincide with the jump point. The choice  $\delta = 0.6$  is consistent with both continuous and discontinuous profiles and this is revealed by the fact that for  $U_c = 10$ , the temperature has a jump, and for both  $U_c = 50$  and  $U_c = 100$  the profile is continuous.

Higher values for  $\delta$ , closer to the limiting value  $2/\gamma$ , give raise to pictures resembling the one already presented in Figure 2 (left column). In particular, the width of the spike region shrinks to a single point.

**Hamer model.** In the case of the system (4) with  $f(s) = \frac{1}{2} s^2$ , if  $g$  is monotone increasing,  $G(0) \leq -1$  if and only if  $c \geq u_-$  and  $G(0) \geq 1$  if and only if  $u_+ \leq c$ . Since  $u_+ < c < u_-$  for any admissible shock wave, discontinuous orbits may appear only as a consequence of the condition  $G'(0) < 2\nu^2$ , that, in the present case, translates into

$$\frac{dg}{du}(c) < \frac{1}{2} \frac{[u]^3}{[g]}.$$

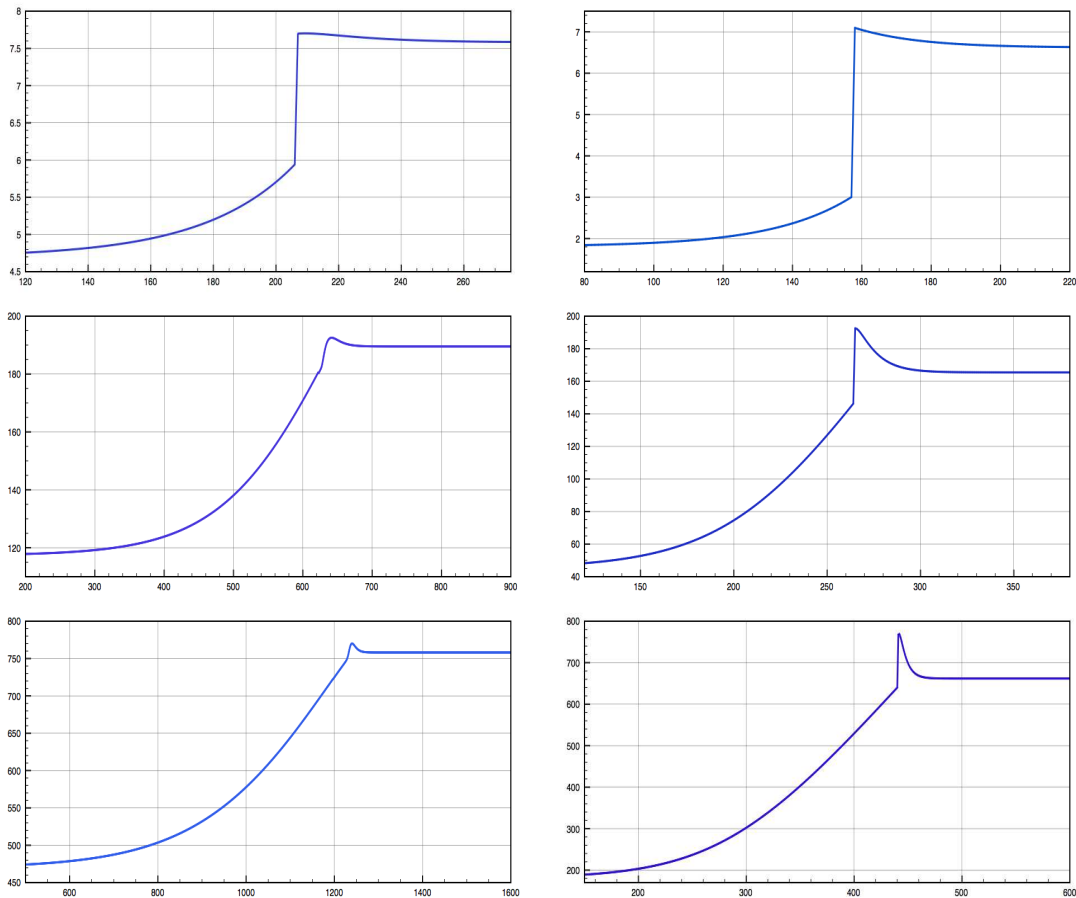


FIGURE 3. Temperature profiles in the cases  $\delta = 0.6$  (left column) and  $\delta = 1.0$  (right column), corresponding to the values  $U_c = 10, 50, 100$  (increasing from top to bottom).

Considering  $g(u) = \sigma u$ ,  $\sigma > 0$ , (see Example (2.1)), the above condition becomes

$$|u_+ - u_-| > \sqrt{2} \sigma,$$

that describes the (sharp) threshold for discontinuous profiles (see [8]).

The case  $g(u) = \sigma u^2$  gives the condition

$$|u_+ - u_-| > 2\sqrt{2} \sigma |c|$$

showing that discontinuous profiles are possible also in the regime of small  $|u_+ - u_-|$ , if the sonic value  $c$  is sufficiently small. Note that in this case, the function  $G$  is non-monotone in  $[-1, 1]$  if and only if

$$|u_+ - u_-| > 2|c|,$$

hence, if  $\sigma > 1/\sqrt{2}$ , both non-monotonicity of  $G$  and continuity of the profile are compatible for some appropriate choice of the asymptotic states  $u_{\pm}$ .

## 5. CONCLUSIONS

The analysis performed shows that shock waves are robust patterns for the system (1) under the assumption (2). Indeed, the existence of such structures is not limited to specific ranges for the asymptotic states; oppositely, they do exist for any regime consistent with the reduced hyperbolic system, obtained by disregarding the radiation effects. Additionally, the system of algebraic-differential system can be dealt with in a rigorous manner with a restricted number of technicalities and, at the same time, with a good number of quantitative informations relative to the internal structure of the shock transition, specifically with respect to the presence of change of monotonicity. This allows to extend the analysis carried out in the region  $\delta \rightarrow 2/\gamma$  in [13] to any regime and gives a sound basis to the result formally derived in [7]. Also, the observation that, for fixed  $\delta$ , the reduced system (3) depends on the value  $|U_+ - U_-|$  (or, equivalently, on  $U_c$ ) as a rotated vector field permits, in principle, to follow the changes in the qualitative properties of the profiles in a “monotone” way with respect to the variation of such value.

The relative simplicity and solidity of the structure of the problem is also revealed from the fact that there is a great freedom in the possible form for the coupling term  $g$  –though the power-like form is the most accredited version– and that there is a reduced number of parameters required to classify different forms for the profiles. More general forms for pressure and internal energy should also preserve the existence of the radiative profiles so that it is reasonable that the results presented in this article extend to more general fluids.

A natural subsequent step is the stability analysis for such radiation profiles, in particular in the presence of spikes. Such problem could be approached taking inspiration from other classes of systems of partial differential equations in the context of conservation laws that support non-monotone traveling wave as in the case of combustion waves. Also, it would be very interesting to analyze the case of radiation hydrodynamics in more general forms and specifically without taking advantage of the assumptions that reduce the model to a hyperbolic-elliptic system of partial differential equations. In particular, considering the native form of a continuous-kinetic coupled model would be a very challenging and stimulating research project.

## REFERENCES

- [1] Buet C.; Després B.; *Asymptotic analysis of fluid models for the coupling of radiation and hydrodynamics*, J. Quant. Spectrosc. Radiat. Transfer 85 (2004) 385–418.
- [2] Coulombel J.-F.; Goudon Th.; Lafitte P.; Lin C.; *Analysis of large amplitude shock profiles for non-equilibrium radiative hydrodynamics: formation of Zeldovich spikes*, preprint, [hal-00593491](#), version 1 - 16 May 2011.
- [3] Duff, G. F. D.; *Limit-cycles and rotated vector fields*, Ann. of Math. (2) 57, (1953) 15–31.
- [4] Gilbarg D.; *The existence and limit behavior of the one-dimensional shock layer*, Amer. J. Math. 73 (1951) no.2, 256–274.
- [5] Godillon-Lafitte P.; Goudon T.; *A coupled model for radiative transfer: Doppler effects, equilibrium and non equilibrium diffusion asymptotics*, SIAM Multiscale Modeling and Simulation 4 (2005) no.4, 1245–1279.
- [6] Hamer K.; *Nonlinear effects on the propagation of sound waves in a radiating gas*, Quart. J. Mech. Appl. Math. 24 (1971), 155–168.

- [7] Heaslet, M.A.; Baldwin, B.S.; *Predictions of the structure of radiation-resisted shock waves*, Phys. Fluids 6 (1963) 781–791.
- [8] Kawashima, S.; Nishibata, S.; *Shock waves for a model system of the radiating gas*, SIAM J. Math. Anal. 30 (1999) no. 1, 95–117.
- [9] Lattanzio C.; Mascia C.; Serre D.; *Shock waves for radiative hyperbolic-elliptic systems*, Indiana Univ. Math. J. **56** (2007) no.5, 2601–2640.
- [10] Lattanzio C.; Mascia C.; Serre D.; *Nonlinear hyperbolic-elliptic coupled systems arising in radiation dynamics*, in “Hyperbolic Problems: Theory, Numerics, Applications (Lyon, July 17-21, 2006)”, S.Benzoni-Gavage and D.Serre, eds., Springer-Verlag, Boston, Berlin, Heidelberg, 2008, 661–669.
- [11] Lin, C.; Coulombel, J.-F.; Goudon, T.; *Shock profiles for non-equilibrium radiating gases*, Phys. D 218 (2006) no. 1, 83–94.
- [12] Lowrie R. B.; Morel J. E.; Hittinger, J. A.; *The coupling of radiation and hydrodynamics*, The Astrophysical J. 521 (1999) 432–450.
- [13] Mihalas, D.; Mihalas, B. W., “Foundations of radiation hydrodynamics”, Oxford University Press, New York, 1984; reprinted by Dover Publications, New York, 1999.
- [14] Perko, L. M.; *Rotated vector fields*, J. Differential Equations 103 (1993), no. 1, 127–145.
- [15] Schochet, S.; Tadmor, E.; *The regularized Chapman-Enskog expansion for scalar conservation laws*, Arch. Rational Mech. Anal. 119 (1992) no. 2, 95–107.
- [16] Zel’dovich, Y. B.; Raizer, Y. P.; “Physics of shock waves and high-temperature hydrodynamic phenomena”, Academic Press, New York, 1967; reprinted by Dover Publications, New York, 2002.

DIPARTIMENTO DI MATEMATICA “G. CASTELNUOVO”, SAPIENZA – UNIVERSITÀ DI ROMA, P.LE ALDO MORO, 2 - 00185 ROMA (ITALY)